BMC Ophthalmology

RESEARCH

Open Access

Varied clinical presentations of *RP1L1* variants in Chinese patients: a study of occult macular dystrophy and vitelliform macular dystrophy

Xiao Liu[1,2,3†], Yanling Long[1,2,3†], Yu Wang[1,2], Bo Liu[1], Jiayun Ren[1,2], Gang wang[1,2], Min Wang[1,2], Xiaohong Meng[1,2,3*] and Yong Liu[1,2,3*]

Abstract

Background Occult Macular Dystrophy (OMD), primarily caused by retinitis pigmentosa 1-like 1 (*RP1L1*) variants, is a complex retinal disease characterised by progressive vision loss and a normal fundus appearance. This study aims to investigate the diverse phenotypic expressions and genotypic correlations of OMD in Chinese patients, including a rare case of Vitelliform Macular Dystrophy (VMD) associated with *RP1L1*.

Methods We analysed seven OMD patients and one VMD patient, all with heterozygous pathogenic *RP1L1* variants. Clinical assessments included Best Corrected Visual Acuity (BCVA), visual field testing, Spectral Domain Optical Coherence Tomography (SD-OCT), multifocal Electroretinograms (mfERGs), and microperimetry. Next-generation sequencing was utilised for genetic analysis.

Results The OMD patients displayed a range of phenotypic variability. Most (5 out of 7) had the *RP1L1* variant c.133 C > T; p.R45W, associated with central vision loss and specific patterns in SD-OCT and mfERG. Two patients exhibited different *RP1L1* variants (c.3599G > T; p.G1200V and c.2880G > C; p.W960C), presenting milder phenotypes. SD-OCT revealed photoreceptor layer changes, with most patients showing decreased mfERG responses in the central rings. Interestingly, a unique case of VMD linked to the *RP1L1* variant was observed, distinct from traditional OMD presentations.

Conclusions This study highlights the phenotypic diversity within OMD and the broader spectrum of *RP1L1*-associated macular dystrophies, including a novel association with VMD. The findings emphasise the complexity of *RP1L1* variants in determining clinical manifestations, underscoring the need for comprehensive genetic and clinical evaluations in macular dystrophies.

Keywords Occult macular dystrophy, *RP1L1* gene, Phenotypic variability, Vitelliform macular dystrophy, Chinese patients, Genetic analysis

†Xiao Liu and Yanling Long contribututed equally to this work.

*Correspondence:
Xiaohong Meng
cqwmwm@163.com
Yong Liu
liuyy99@163.com

[1]Department of Ophthalmology, Southwest Hospital of Army Medical University, Chongqing 400038, China
[2]Key Lab of Visual Damage and Regeneration & Restoration of Chongqing, Chongqing 400038, China
[3]Jinfeng Laboratory, Chongqing 401239, China

Background

Retinitis pigmentosa 1-like 1 gene (*RP1L1*, OMIM: 608,581), located on chromosome 8, encodes a component of the photoreceptor axoneme. A 1167-bp region between positions 5968 and 7135 in the *RP1L1* gene encodes 25 imperfect copies of a 16-amino acid repeat module. This region has a high GC content of 62%, making it less efficiently amplifiable by polymerase chain reaction (PCR) from both RNA and genomic DNA [1]. As its name suggests, *RP1L1* is highly similar to the retinitis pigmentosa 1 (encoded by *RP1*, OMIM: 603,937) gene. *RP1* and *RP1L1* are predicted to be integral to the development and maintenance of the outer segment of photoreceptors, playing a pivotal role in transporting materials between the inner and outer segments, thereby maintaining the biochemical homeostasis of the photoreceptor [2, 3]. Pathogenic variants in *RP1L1* lead to progressive photoreceptor degenerative disorders like autosomal dominant occult macular dystrophy (OMD, OMIM: 613,587) and autosomal recessive retinitis pigmentosa 88 (RP88, OMIM: 618,826) [4–7]. OMD typically presents with slowly progressive visual disturbances, a normal-appearing fundus, and selective abnormalities in the photoreceptor layer observable through optical coherence tomography (OCT) [8, 9]. SD-OCT provides valuable in vivo information about the microstructure of photoreceptors in OMD. Two primary pathophysiological types of OMD have been identified [8, 10–12]: classical OMD, characterised by both blurred ellipsoid zone (EZ) and absence of the interdigitation zone (IZ) on SD-OCT, and subtle OMD, where at least one of these features is absent. The clinical presentation of OMD can be categorised into three stages based on the degree of IZ and EZ involvement, potentially correlating with the duration of disease onset [13, 14].

OMD was previously considered the only maculopathy caused by *RP1L1* deficiency, characterised by a normal fundus. However, recent studies have identified additional phenotypes, such as adult-onset pseudo-vitelliform macular dystrophy (VMD) and conditions resembling Best disease [9, 15]. These discoveries have introduced the term "*RP1L1* maculopathy" to describe the broader spectrum of maculopathies associated with *RP1L1* variants.

The purpose of this study is to characterise the clinical and molecular genetic features of a cohort with OMD and a VMD caused by heterozygous pathogenic *RP1L1* variants in Chinese patients.

Methods

Clinical assessment

Clinical data were collected from patients with variants in the *RP1L1* gene. Examinations were conducted after obtaining written informed consent and in accordance with the principles of the Declaration of Helsinki. The procedures used in this study were approved by the local ethics committee of Southwest Hospital, Army Medical University, Chongqing, China (reference number: KY2023007). Detailed medical history and comprehensive ophthalmological examinations were performed, including decimal best-corrected visual acuity (BCVA), color fundus photography, spectral domain optical coherence tomography (SD-OCT, Heidelberg and Zeiss), fundus autofluorescence imaging (FAF; excitation: 488 nm, Spectralis HRA+OCT; Heidelberg Engineering, Dossenheim, Germany), Humphrey's visual fields (HVFs, 30−2) and microperimetry (MP) (MAIA, 4−2, Italy and NIDEK, MP3, Japan). We recorded full-field electroretinograms (ffERGs) (Espion E2, Diagnosys LLC, Lowell, MA, USA and MonPack 3, Metrovision, France) following the standards of the International Society for Clinical Electrophysiology of Vision (ISCEV). Multifocal ERGs (mfERGs) were recorded with a VERIS Science 6.3.2 imaging system (103-hexagon, EDI, San Mateo, CA) in accordance with the ISCEV standard protocol. The mfERGs with stable fixation were selected for further analysis.

Two subtypes of SD-OCT morphologic phenotype were applied to describe the structural changes according to a previous study [8]: (1) severe phenotype (denoted as a classical phenotype compatible with stages IIa, IIb, IIIa and IIIb), showing both blurred/flat EZ and absence of IZ; and (2) mild phenotype (denoted as subtle morphologic changes compatible to stage Ia, Ib), defined as minimal/local blurring of EZ and local absence of IZ.

The P1 amplitude decrease rate was calculated by comparing the amplitude of the P1 component in patients to a normal reference. This calculation was executed using the formula: (Normal P1 - Patient P1) / Normal P1. Values less than 10% were considered negligible and recorded as zero.

Pathogenic variant detection

Peripheral venous blood samples were collected from all subjects and unaffected family members for Genomic DNA extraction using standard procedure. Either eye gene-enriched (97 to 384 IRD genes) panel-based next-generation sequencing (NGS) or whole exome sequencing (WES) was performed. The raw reads were aligned to the human reference genome (GRCh38/hg38) using the Burrows Wheeler Aligner tool. Sequencing data processing and bioinformatics analysis followed the methods of Meng et al. [16]. Sanger sequencing (the primers are listed in Supplementary Table 1) was used to perform co-segregation analysis of candidate pathogenic variants. The pathogenicity of the candidate pathogenic variants were assessed according to the American College of Medical Genetics and Genomics (ACMG) guidelines.

Table 1 Summary of clinical characteristics and *RP1L1*[#] variants in seven OMD patients

Patient NO.	Family NO.	Sex	Age		Initial symptoms	BCVA (LogMAR)		Funduscopy	OCT	Visual Field	Nucleotide substitution	Amino acid change	Hom/Het
			Onset	diagnosis		RE	LE						
Pt.1	1	M	5	5	Ruduced VA	0.82	0.82	Normal	classical (IIIa)	CS	c.133 C>T	p.R45W	Het
Pt.2	1	F	38	38	Ruduced VA	0.70	0.70	Normal	classical (IIb)	CS	c.133 C>T	p.R45W	Het
Pt.3	1	M	19	69	Ruduced VA	NA	NA	Normal	classical (IIa)	CS	c.133 C>T	p.R45W	Het
Pt.4	2	M	0	30	Ruduced VA	0.82	0.82	Normal	classical (IIIa)	CS	c.133 C>T	p.R45W	Het
Pt.5	3	F	6	11	Ruduced VA	0.70	0.70	Normal	classical (IIIa)	CS	c.133 C>T	p.R45W	Het
Pt.6	4	M	38	48	Abnormal color vison	0.40	0.40	Normal	classical (IIIa)	CS	c.3599G>T	p.G1200V	Het
Pt.7	5	M	57	57	No symptoms	0.05	0.05	Normal	Subtle (IIb)	NA	c.2880G>C	p.W960C	Het

[#] The transcripts of the *RP1L1* we used in this study for sequencing and reference was NM_178857.6; F: Famale; M: Male; VA: Visual acuity; BCVA: Best-corrected visual acuity; CS: Central scotoma; NA: not available

Results

Traditional phenotype caused by *RP1L1* variant: occult macular dystrophy

We identified seven individuals from five families diagnosed with OMD, all harboring heterozygous pathogenic *RP1L1* variants (Fig. 1). These patients exhibited normal fundus appearance but had central scotomas in their visual fields. They ages at the last examination ranged from 5 to 69 years, with onset ages between 0 and 57 years. The median BCVA was 0.7 (range: 0.05 to 0.82) in logMAR units. Genetic testing revealed the heterozygous variant c.133 C>T; p.R45W in five out of seven OMD patients, while two patients had the heterozygous variants c.3599G>T; p.G1200V and c.2880G>C; p.W960C, respectively (Table 1). According to the ACMG guidelines, these three variants were classified as pathogenic, likely pathogenic and pathogenic, respectively (Supplementary Table 2). Patients 6 and 7 exhibited a milder phenotype, as evident in BCVA, mfERGs and microperimetric assessments (Fig. 2).

SD-OCT showed morphologic changes in the photoreceptor layers. Six out of seven OMD patients demonstrated blurring of the EZ and absence of the IZ in both eyes. Patient 7, however, had a preserved foveal structure with blurred and interrupted EZ and IZ in the parafoveal regions. Other retinal layers, including the outer nuclear layer (ONL) and retinal pigment epithelium (RPE), appeared normal. Patients were classified into SD-OCT stages based on spatial functional and morphological features (Fig. 2).

A decrease in mfERGs across six eccentric rings was observed in both eyes of most patients. Except for Patient 7, all showed significantly lower responses in the central rings (Fig. 3).

In terms of preferred retinal loci (PRLs), seven eyes from four OMD patients with the R45W variant were assessed. Two PRLs were located within the central macula, while five were outside. The two with central PRLs exhibited similar mean microperimetry sensitivity (MS) at the fovea and parafovea. Patient 6, with the G1200V variant, showed stable fixation at the fovea with lower MS, while Patient 7, with the W960C variant, displayed normal MS at the macula (Table 2).

A special phenotype caused by *RP1L1* variant: vitelliform macular dystrophy

Patient 8, a 30-year-old male, experienced progressive central visual loss in both eyes over four years. There were no reports of systemic diseases, trauma, drug abuse, smoking or consanguineous marriage in his family. His BCVA was 0.82 and 1.00 in the right and left eyes, respectively. Fundus imaging showed bright, yellow vitelliform deposits at the macula in both eyes (Fig. 4a). SD-OCT scans indicated abnormal thickening in the foveal

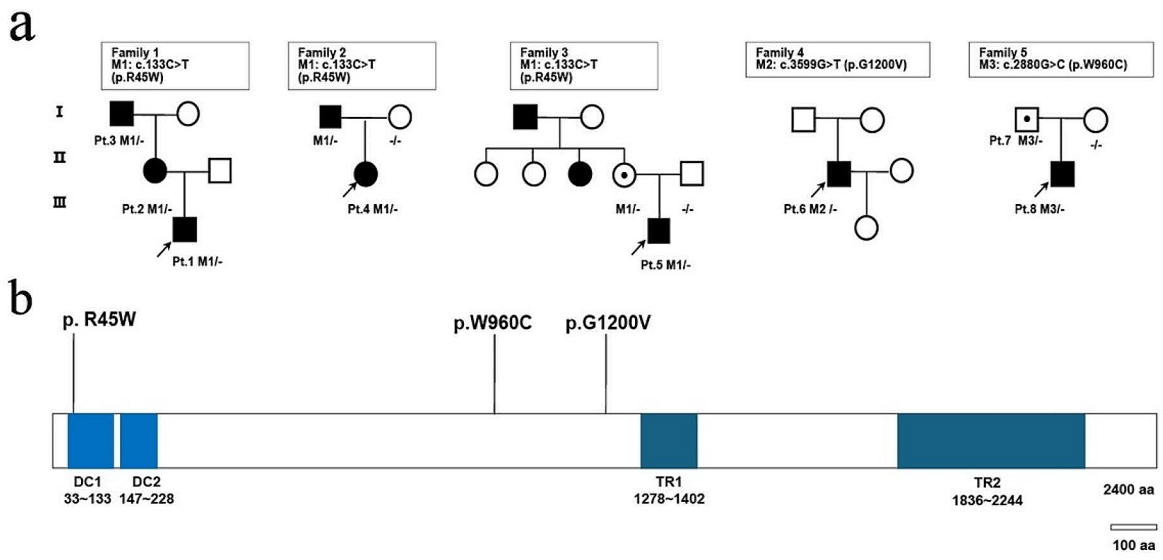

Fig. 1 **a** Pedigrees of five families affected by OMD and harboring heterozygous pathogenic *RP1L1* variants. Affected individuals are represented by solid squares (men) and circles (women), while unaffected members are indicated with white icons. The proband in each family is identified with an arrow. The presence of wild type is denoted by "-". Generation numbers are indicated on the left. M1, M2 and M3 correspond to the *RP1L1* variants p.R45W, p.G1200V, and p.W960C, respectively. **b** Illustration of the location of these three variants within the genetic and protein structures of *RP1L1*.

region. MfERGs showed a marked decrease in central response, with peripheral functions relatively preserved. EOGs displayed normal Arden ratios, and ffERGs were normal (Supplementary Table 3).

Patient 7, a 57-year-old, the father of the aforementioned patient, had no visual complaints. His BCVA was 0.05 in both eyes. Fundus images and autofluorescence appeared normal (Fig. 4b). SD-OCT showed a preserved foveal structure with blurred and interrupted EZ and IZ in the parafoveal regions. MfERGs indicated a slight central reduction in function but preserved peripheral function. ffERGs were normal (Supplementary Table 3).

Discussion

The results of this study, contextualised within the current understanding of *RP1L1*-associated macular dystrophies, underscore the considerable variability and complexity in the clinical presentation and genetic underpinnings of these conditions. Our findings of seven affected individuals from five families, all harboring heterozygous pathogenic *RP1L1* variants and presenting with OMD phenotypes (classical and subtle), align with established patterns of *RP1L1* variants leading to progressive photoreceptor degeneration [8, 13, 14, 17].

In our cohort, the majority of OMD patients had the *RP1L1* variants c.133 C>T; p.R45W. This finding is consistent with previous studies where this variant was identified as a common causative factor in OMD irrespective of ethnic or genetic backgrounds [11, 18–23]. This variant was particularly associated with worse BCVA, distinctive SD-OCT and mfERG findings, highlighting its significant clinical impact [14, 19, 23–26].

Our study further categorises OMD into clinical stages based on photoreceptor structures observed in OCT images. Most patients showed decreased amplitude in the center area observed in mfERGs, indicating disease progression with central involvement. We also analysed microperimetric features in OMD patients, revealing PRLs in most eyes of patients with the R45W variant. Despite relatively normal MS, abnormalities in microperimetry at the fovea and central area were evident, correlating with BCVA, OCT structure, and mfERG findings. Patients with G1200V and p.W960C variants exhibited good fixation, and Patient 7 showed normal MP at the macula, compatible with his good vision, central macular structure, and normal mfERGs. This comprehensive approach underscores the importance of integrating various diagnostic modalities to fully understand the spectrum of *RP1L1*-associated OMD.

The identification of a patient presenting with VMD due to an *RP1L1* variant in our study adds another layer of complexity to the phenotypic spectrum of *RP1L1* variants. This is the first case reported in the Chinese population, resonating with recent descriptions of "*RP1L1*

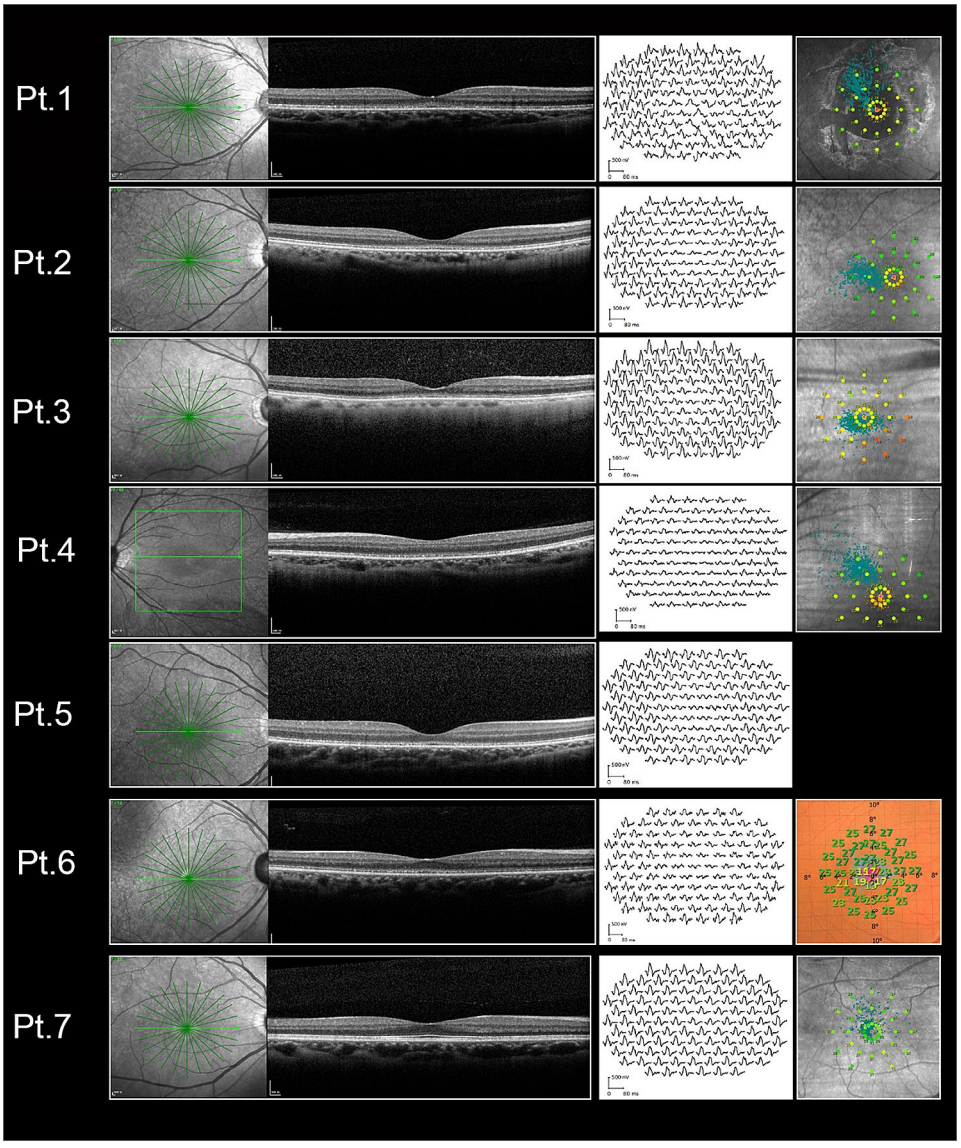

Fig. 2 Displays SD-OCT, mfERGs, and Microperimetry results for one eye of each of the seven OMD patients, who experienced a symmetrical bilateral decline in visual acuity

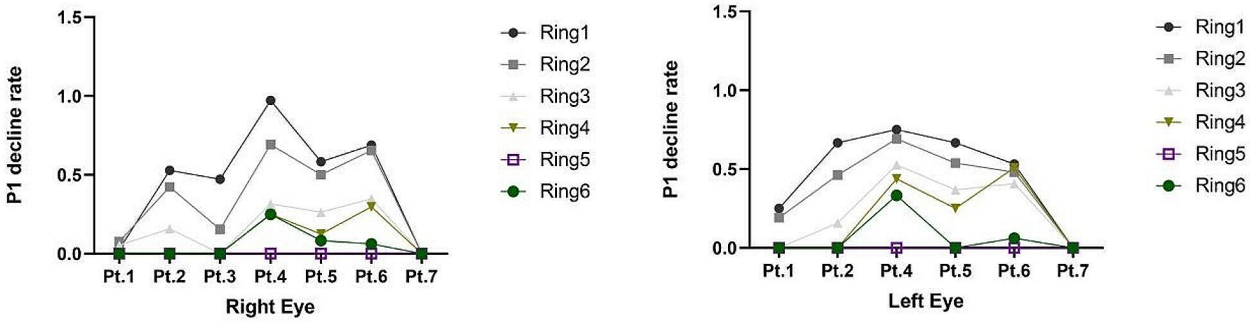

Fig. 3 Decline rate in mfERGs responses across six eccentric rings in both eyes of the patients. The left eye of Patient 3 was omitted due to poor fixation. All patients, except for Patient 7, exhibited significantly lower response densities in rings 1 and 2

Table 2 Microperimetric features of the OMD patients

Patient NO.	BCEA(^{o2})				Fovea. Thresh. (dB)		Para-fovea(2°) Aver. Thresh. (dB)		Aver. Thresh. (dB)	
	RE(63%)	LE(63%)	RE(95%)	LE(95%)	RE	LE	RE	LE	RE	LE
Pt.1	6.6	7.3	59.3	65.7	18	16	22.5	22.1	24.5	23.8
Pt.2	4.5	3	40.5	26.8	20	22	23.3	22.5	25.9	26
Pt.3	2.8	NA	25.3	NA	22	NA	22.5	NA	21.8	NA
Pt.4	2	6.5	18	58.5	23	21	21.5	20.9	24	25.1
Pt.6	2.5	2.1	6.7(95.4%)	5.8(95.4%)	17	15	22.3	22.5	23.6	22.2
Pt.7	2.5	1.7	22.6	15.2	27	25	28.7	29.2	27.6	28.4

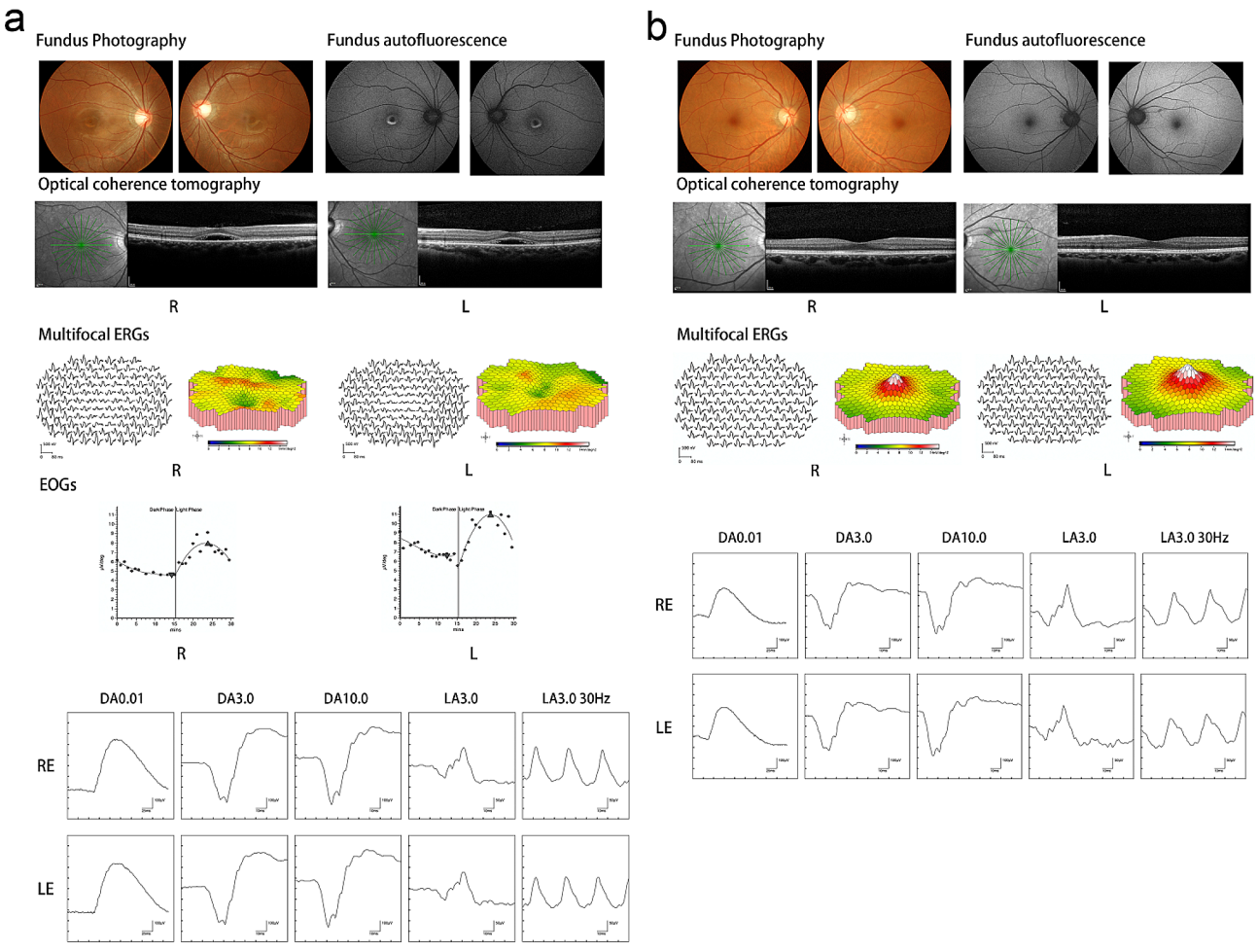

Fig. 4 **a** The clinical presentation of Patient 8, who exhibited the phenotype of Vitelliform Macular Dystrophy (VMD). **b** The clinical presentation of Patient 8's father (Patient 7), who exhibited the phenotype of Occult Macular Dystrophy (OMD).

maculopathy" where visible maculopathy resembling adult-onset pseudovitelliform macular dystrophy or Best disease was observed in two reports [9, 15]. Our study extends this observation, indicating that *RP1L1* variants can manifest in a broader array of phenotypes than previously recognised. Interestingly, the patient's father (Pt. 7), who carries the same *RP1L1* variant, showed an OMD phenotype, suggesting a broader spectrum of *RP1L1*-associated pathologies.

The variability in clinical presentations and the severity of phenotypes observed in our cohort, along with the established understanding that *RP1L1* gene expression plays a crucial role in photoreceptor morphogenesis, suggest a complex interplay between genetic factors and phenotypic expression. Our observations align with the largest genetically confirmed East Asian cohort study, which identified three functional phenotypes based on mfERG abnormalities, demonstrating the wide spectrum of functional and structural damage associated with

RP1L1 Variants [14, 27]. The study also emphasised the importance of assessing the EZ line in OCT for identifying functional subtypes and disease severity, a finding that resonates with our observations.

In conclusion, our study not only reaffirms the genetic and clinical diversity of *RP1L1* maculopathy but also expands the known phenotype spectrum. It reinforces the need for heightened awareness among clinicians and researchers about the broad spectrum of phenotypes associated with *RP1L1* variants and the importance of genetic testing for accurate diagnosis and management of these complex conditions. The findings have significant implications for patient management and future research.

Supplementary Information

The online version contains supplementary material available at https://doi.org/10.1186/s12886-024-03591-7.

Supplementary Material 1

Supplementary Material 2

Supplementary Material 3

Acknowledgements

The authors thank the patients and their families for participation in this study; Prof. Kaoru Fujinami and Dr. Yu Fujinami-Yokokawa, the National Institute of Sensory Organs, the National Tokyo Medical Center, Japan, for help in clinical and genetic data analysis.

Author contributions

XL and YL collected the data and wrote the main manuscript. YW, BL, JR, GW and MW interpreted the patient data. YL and XM designed the work and substantively revised the manuscript. All authors reviewed the manuscript and approved the final manuscript.

Data availability

The datasets generated and/or analysed during the current study are available from the corresponding author on reasonable request.

Declarations

Ethics approval and consent to participate

All procedures performed in studies involving human participants were adhered to the World Medical Association Declaration of Helsinki. This study protocol was reviewed and approved by the local ethics committee of Southwest Hospital, Army Medical University, Chongqing, China (reference number: KY2023007). Informed consent was obtained for each participant in this study. For participant with age less than 16, we also have obtained informed consent from their respective parent(s)/guardian(s).

Consent for publication

Written informed consent has been obtained from each participant to publish this paper. For participant with age less than 16, we also have obtained consent from their respective parent(s)/guardian(s).

Competing interests

The authors declare no competing interests.

Received: 24 February 2024 / Accepted: 24 July 2024
Published online: 06 August 2024

References

1. Conte I, Lestingi M, den Hollander A, Alfano G, Ziviello C, Pugliese M, Circolo D, Caccioppoli C, Ciccodicola A, Banfi S. Identification and characterisation of the retinitis pigmentosa 1-like1 gene (*RP1L1*): a novel candidate for retinal degenerations. Eur J Hum Genet. 2003;11(2):155–62.
2. Yamashita T, Liu J, Gao J, LeNoue S, Wang C, Kaminoh J, Bowne SJ, Sullivan LS, Daiger SP, Zhang K, et al. Essential and synergistic roles of *RP1* and *RP1L1* in rod photoreceptor axoneme and retinitis pigmentosa. J Neurosci. 2009;29(31):9748–60.
3. Bowne SJ, Daiger SP, Malone KA, Heckenlively JR, Kennan A, Humphries P, Hughbanks-Wheaton D, Birch DG, Liu Q, Pierce EA, et al. Characterization of *RP1L1*, a highly polymorphic paralog of the retinitis pigmentosa 1 (*RP1*) gene. Mol Vis. 2003;9:129–37.
4. Miyake Y, Ichikawa K, Shiose Y, Kawase Y. Hereditary Macular dystrophy without visible fundus abnormality. Am J Ophthalmol. 1989;108(3):292–9.
5. Miyake Y, Horiguchi M, Tomita N, Kondo M, Tanikawa A, Takahashi H, Suzuki S, Terasaki H. Occult macular dystrophy. Am J Ophthalmol. 1996;122(5):644–53.
6. Akahori M, Tsunoda K, Miyake Y, Fukuda Y, Ishiura H, Tsuji S, Usui T, Hatase T, Nakamura M, Ohde H, et al. Dominant mutations in *RP1L1* are responsible for occult macular dystrophy. Am J Hum Genet. 2010;87(3):424–9.
7. Davidson AE, Sergouniotis PI, Mackay DS, Wright GA, Waseem NH, Michaelides M, Holder GE, Robson AG, Moore AT, Plagnol V, et al. *RP1L1* variants are associated with a spectrum of inherited retinal diseases including retinitis pigmentosa and occult macular dystrophy. Hum Mutat. 2013;34(3):506–14.
8. Nakamura N, Tsunoda K, Mizuno Y, Usui T, Hatase T, Ueno S, Kuniyoshi K, Hayashi T, Katagiri S, Kondo M, et al. Clinical stages of Occult Macular dystrophy based on Optical Coherence Tomographic findings. Invest Ophthalmol Vis Sci. 2019;60(14):4691–700.
9. Noel NCL, MacDonald IM. *RP1L1* and inherited photoreceptor disease: a review. Surv Ophthalmol. 2020;65(6):725–39.
10. Miyake Y, Tsunoda K. Occult macular dystrophy. Jpn J Ophthalmol. 2015;59(2):71–80.
11. Park SJ, Woo SJ, Park KH, Hwang JM, Chung H. Morphologic photoreceptor abnormality in occult macular dystrophy on spectral-domain optical coherence tomography. Invest Ophthalmol Vis Sci. 2010;51(7):3673–9.
12. Viana KÍ, Messias A, Siqueira RC, Rodrigues MW, Jorge R. Structure-functional correlation using adaptive optics, OCT, and microperimetry in a case of occult macular dystrophy. Arq Bras Oftalmol. 2017;80(2):118–21.
13. Tsunoda K, Hanazono G. Detailed analyses of microstructure of photoreceptor layer at different severities of occult macular dystrophy by ultrahigh-resolution SD-OCT. Am J Ophthalmol Case Rep. 2022;26:101490.
14. Yang L, Joo K, Tsunoda K, Kondo M, Fujinami-Yokokawa Y, Arno G, Pontikos N, Liu X, Nakamura N, Kurihara T, et al. Spatial functional characteristics of east Asian patients with Occult Macular dystrophy (Miyake Disease); EAOMD Report 2. Am J Ophthalmol. 2021;221:169–80.
15. Manayath GJ, Rokdey M, Verghese S, Ranjan R, Saravanan VR, Narendran V. An extended phenotype of *RP1L1* maculopathy - case report. Ophthalmic Genet. 2022;43(3):392–9.
16. Meng XH, Long YL, Ren JY, Wang G, Yin X, Li SY. Ocular characteristics of patients with Bardet-Biedl Syndrome caused by pathogenic *BBS* Gene Variation in a Chinese cohort. Front Cell Dev Biol. 2021;9:635216.
17. Luoma-Overstreet G, Jewell A, Brar V, Couser N. Occult Macular dystrophy: a case report and major review. Ophthalmic Genet. 2022;43(5):703–8.
18. Zabek O, Lamprakis I, Rickmann A, Calzetti G, György B, Scholl HPN, Della Volpe Waizel M. Rare occult macular dystrophy with a pathogenic variant in the *RP1L1* gene in a patient of Swiss descent. Am J Ophthalmol Case Rep. 2022;26:101527.
19. Wang DD, Gao FJ, Li JK, Chen F, Hu FY, Xu GZ, Zhang JG, Sun HX, Zhang SH, Xu P, Tian GH, Wu JH. Clinical and Genetic Characteristics of Chinese Patients with Occult Macular dystrophy. Invest Ophthalmol Vis Sci. 2020;61(3):10.
20. Fujinami K, Yang L, Joo K, Tsunoda K, Kameya S, Hanazono G, Fujinami-Yokokawa Y, Arno G, Kondo M, Nakamura N, Kurihara T, Tsubota K, Zou X, Li H, Park KH, Iwata T, Miyake Y, Woo SJ, Sui R. East Asia Inherited Retinal Disease Society study group. Clinical and genetic characteristics of east Asian patients with Occult Macular dystrophy (Miyake Disease): East Asia Occult Macular dystrophy Studies Report Number 1. Ophthalmology. 2019;126(10):1432–44.
21. Zobor D, Zobor G, Hipp S, Baumann B, Weisschuh N, Biskup S, Sliesoraityte I, Zrenner E, Kohl S. Phenotype variations caused by mutations in the *RP1L1* gene in a large mainly German cohort. Invest Ophthalmol Vis Sci. 2018;59(7):3041–52.

22. Qi YH, Gao FJ, Hu FY, Zhang SH, Chen JY, Huang WJ, Tian GH, Wang M, Gan DK, Wu JH, Xu GZ. Next-generation sequencing-aided Rapid Molecular Diagnosis of Occult Macular Dystrophy in a Chinese family. Front Genet. 2017;8:107.
23. Ahn SJ, Cho SI, Ahn J, Park SS, Park KH, Woo SJ. Clinical and genetic characteristics of Korean occult macular dystrophy patients. Invest Ophthalmol Vis Sci. 2013;54(7):4856–63.
24. Ruan MZ, Hussnain SA, Thomas A, Mansukhani M, Tsang S, Yannuzzi L. Utility of en-face imaging in diagnosis of occult macular dystrophy with *RP1L1* mutation: a case series. Am J Ophthalmol Case Rep. 2019;15:100465.
25. Fu Y, Chen KJ, Lai CC, Wu WC, Wang NK. Clinical features in a case of occult macular dystrophy with *RP1L1* mutation. Retin Cases Brief Rep. 2019;13(2):158–61.
26. Fujinami K, Kameya S, Kikuchi S, Ueno S, Kondo M, Hayashi T, Shinoda K, Machida S, Kuniyoshi K, Kawamura Y, Akahori M, Yoshitake K, Katagiri S, Nakanishi A, Sakuramoto H, Ozawa Y, Tsubota K, Yamaki K, Mizota A, Terasaki H, Miyake Y, Iwata T, Tsunoda K. Novel RP1L1 variants and genotype-photoreceptor Microstructural phenotype associations in Cohort of Japanese patients with Occult Macular dystrophy. Invest Ophthalmol Vis Sci. 2016;57(11):4837–46.
27. Ahn SJ, Yang L, Tsunoda K, Kondo M, Fujinami-Yokokawa Y, Nakamura N, Iwata T, Kim MS, Mun Y, Park JY, Joo K, Park KH, Miyake Y, Sui R, Fujinami K, Woo SJ, East Asia Inherited Retinal Disease Society Study Group. Visual field characteristics in east Asian patients with Occult Macular dystrophy (Miyake Disease): EAOMD Report 3. Invest Ophthalmol Vis Sci. 2022;63(1):12.

Publisher's Note